HHS Public Access

Author manuscript

J Biomed Mater Res A. Author manuscript; available in PMC 2020 December 09.

Published in final edited form as:

J Biomed Mater Res A. 2020 October ; 108(10): 2123–2132. doi:10.1002/jbm.a.36971.

Creation of a contractile biomaterial from a decellularized spinach leaf without ECM protein coating: An in vitro study

Emily R. Robbins[1], **George D. Pins**[1], **Michael A. Laflamme**[2], **Glenn R. Gaudette**[1]

[1]Biomedical Engineering, Worcester Polytechnic Institute, Worcester, Massachusetts

[2]McEwen Stem Cell Institute, University Health Network, Toronto, Ontario, Canada

Abstract

Myocardial infarction (MI) results in the death of cardiac tissue, decreases regional contraction, and can lead to heart failure. Tissue engineered cardiac patches containing human induced pluripotent stem cell-derived cardiomyocytes (hiPS-CMs) can restore contractile function. However, cells within thick patches require vasculature for blood flow. Recently, we demonstrated fibronectin coated decellularized leaves provide a suitable scaffold for hiPS-CMs. Yet, the necessity of this additional coating step is unclear. Therefore, we compared hiPS-CM behavior on decellularized leaves coated with collagen IV or fibronectin extracellular matrix (ECM) proteins to non-coated leaves for up to 21 days. Successful coating was verified by immunofluorescence. Similar numbers of hiPS-CMs adhered to coated and noncoated decellularized leaves for 21 days. At Day 14, collagen IV coated leaves contracted more than non-coated leaves (3.25 ± 0.39% vs. 1.54 ± 0.60%; $p < .05$). However, no differences in contraction were found between coated leaves, coated tissue culture plastic (TCP), noncoated leaves, or noncoated TCP at other time points. No significant differences were observed in hiPS-CM spreading or sarcomere lengths on leaves with or without coating. This study demonstrates that cardiac scaffolds can be created from decellularized leaves without ECM coatings. Noncoated decellularized leaf surfaces facilitate robust cell attachment for an engineered tissue patch.

Keywords

decellularized leaves; extracellular matrix; high-speed imaging; mechanical contraction; pluripotent stem cell-derived cardiomyocytes

1 | INTRODUCTION

Cardiovascular disease (CVD) is the leading cause of death worldwide (Benjamin, Blaha, Chiuve, & Cushman, 2017). Myocardial infarction (MI) results from occlusion in a coronary artery, leading to tissue ischemia, cell death, and replacement by fibrotic scar (Czirok et al., 2017; Rodness et al., 2016). MI due to coronary artery disease is generally a regional

Correspondence Glenn R. Gaudette. Biomedical Engineering, Worcester Polytechnic Institute, 100 Institute Rd., Worcester, MA 01609. gaudette@wpi.edu.

SUPPORTING INFORMATION

Additional supporting information may be found online in the Supporting Information section at the end of this article.

disease, resulting in decreased contraction in part of the heart. If a significant amount of tissue is infarcted, overall cardiac function will decrease. When the metabolic demand of the body is not met, heart failure occurs. For patients with advanced heart failure, a heart transplant is often the only solution to restore contractile function; however, the number of available donor organs does not meet the need of patients requiring a transplant (Colvin et al., 2017; Czirok et al., 2017; Yancy et al., 2013).

As MI is often the cause of heart failure, restoring contractile function to the infarcted region of the heart may restore enough cardiac function to enable the heart to meet the metabolic demand of the body. A tissue engineered implantable patch could improve function of the infarcted heart, providing an alternative to cardiac transplantation. One challenge is supplying tissues with adequate nutrients and waste removal with a vascular system to maintain viability. Vasculature is required because cells are only able to survive a maximum of 200 μm from a nutrient source due to limitations of oxygen diffusion (Mao & Mooney, 2015; Riemenschneider et al., 2016). A possible solution to this challenge is to utilize a biocompatible biomaterial scaffold that has an intrinsic vascular system for a cardiac tissue patch.

Previous research showed that vascularized mammalian organs and tissues can be decellularized and used as tissue engineered scaffolds (Gershlak et al., 2017; Guyette et al., 2016; Ott et al., 2008; Song & Ott, 2011). Decellularized mammalian cardiac tissue retains the complex material properties and structure of the heart and native vasculature (Gershlak et al., 2017; Guyette et al., 2014; Guyette et al., 2016; Matsuda et al., 2013; Ott et al., 2008; Shevach, Soffer-Tsur, Fleischer, Shapira, & Dvir, 2014) and can be repopulated with cells (Guyette et al., 2016; Ott et al., 2008; Parsa, Ronaldson, & Vunjak-Novakovic, 2016; Schwan et al., 2016; Williams, Quinn, Georgakoudi, & Black, 2014). However, these scaffolds can be expensive and prohibitive since there are a limited number of available mammalian tissues.

Recently, we demonstrated the use of a decellularized spinach leaf as a vascularized cardiac patch scaffold (Gershlak et al., 2017). Spinach leaves are inexpensive, have no associated donor costs, and are biocompatible. The primary remaining scaffold after leaf perfusion-based decellularization is cellulose, a biomaterial used for a variety of medical applications (Czaja, Young, Kawecki, & Brown, 2007; Entcheva et al., 2004; Modulevsky, Cuerrier, & Pelling, 2016). Spinach leaves also have an inherent vascular network, which remains patent after decellularization (Gershlak et al., 2017), and plant vascular branching is similar to that of the human cardiovascular system (McCulloh, Sperry, & Adler, 2003). As such, decellularized leaves have several properties that make them ideal candidates for a cardiac patch scaffold.

Initial studies showed that decellularized leaves coated with fibronectin, an extracellular matrix (ECM) protein found in adult cardiac ECM, are effective for cardiomyocyte adherence and function (Gershlak et al., 2017). Other ECM proteins can also be used to coat biomaterials for cardiac applications. We demonstrated collagen IV coated fibrin microthreads provide a surface conducible for cardiomyocyte adherence and function (Hansen, Laflamme, & Gaudette, 2018). However, as ECM proteins are sourced from

allogeneic donors, protein sourcing and processing are serious concerns that must be considered for clinical translation. Furthermore, minimizing required materials will reduce production costs, complexity, and potential deviations in the manufacturing process, which are important considerations for clinical translation and product manufacturing. Ideally, tissue scaffolds should not require ECM surface coatings for cardiomyocyte function. To determine whether ECM coatings are necessary and improve hiPS-CM behavior on leaf scaffolds, we compared hiPS-CM adherence, maturation, and contractile function on ECM and non-ECM coated decellularized leaves.

2 | MATERIALS AND METHODS

2.1 | Spinach decellularization

Spinach leaves were obtained from the market and the leaf stem cannulated with 27 gauge needles. Leaves were treated three times serially with hexanes (98%, Mixed Isomers, Alfa Aesar, Haverhill, MA) and 1X phosphobuffered saline (PBS) to remove the cuticle layer from the leaf's surface. Cannulated leaves were decellularized using perfusion techniques, as previously described, at a constant pressure head of 152 mmHg (Gershlak et al., 2017). Solutions of 1% sodium dodecyl sulfate (SDS) in deionized (DI) water, followed by 0.1% Triton-X-100/10% bleach in DI water, and lastly DI water were perfused through leaf stems, each for 24 hours. Leaf scaffolds were rinsed in 10 mM Tris buffer pH 9.0 overnight on a shaker plate, frozen at −20°C, and lyophilized. Lyophilized leaves were stored at room temperature until use.

2.2 | Leaf scaffold surface coating

After decellularization and lyophilization, 4 cm^2 sections of decellularized spinach leaves were rehydrated on a shaker plate with 10 mM Tris buffer pH 9.0 solution, rinsed with DI water, and sterilized with 70% ethanol, each for 30 minutes. Leaves in 70% ethanol were transferred into a biosafety cabinet and rinsed three times in sterile 1X PBS. Leaves were incubated at 37°C in RPMI-B27 cell media (RPMI, 2% B27, 1% L-glutamine, and 1% Penicillin/Streptomycin) overnight. After incubation, RPMI-B27 media was aspirated from the decellularized leaves and sterile 10 mm diameter Pyrex cloning wells (Corning Inc., Corning, NY) were positioned on the leaf surface. Sterile 100 μl solutions of fibronectin (human plasma, 100 μg/ml, Sigma Aldrich), collagen IV (human placenta, 10 μg/ml, Sigma Aldrich), or 1X PBS (no coating) were pipetted into the cloning wells. Fibronectin and collagen IV protein concentrations were determined by previous studies in which we had successful cardiomyocyte adherence and contraction on decellularized leaves (Gershlak et al., 2017) and fibrin microthreads (Hansen et al., 2018). In preliminary studies, 100 μg/ml fibronectin coating on leaves resulted in improved cardiomyocyte adherence compared to 10 μg/ml; therefore, this study proceeded with 100 μg/ml. Coatings on leaves were air dried at room temperature in a biosafety cabinet until dry.

ECM coatings on leaves were verified with immunofluorescence antibody staining and imaging. After coating, samples were fixed in 4% paraformaldehyde and immunolabeled for fibronectin (rabbit anti-human, Abcam) or collagen IV (mouse anti-human, Abcam) primary antibodies and Alexa Fluor 488 goat anti-rabbit or anti-mouse secondary antibodies,

respectively (Figure S1). Samples were then imaged with a scanning confocal microscope (Leica Microsystems, Buffalo Grove, IL).

2.3 | hiPS-CM differentiation, isolation, and seeding on leaves

A contractile cardiac patch composed of hiPS-CMs on decellularized spinach leaves has the potential to improve diseased cardiac tissue function following MI. hiPS-CMs were formed by genetically reprogramming adult somatic cells to exhibit characteristics of embryonic stem cells (Takahashi & Yamanaka, 2006; Yu, Smuga-Otto, Vodyanik, et al., 2007), and differentiated into cardiomyocytes with induction of activin-A and bone morphogenetic protein-4, as previously described (Kattman et al., 2011; Yang et al., 2008). Cells were cryopreserved, with cell preparations contained >75% cardiomyocytes, determined by cardiac troponin T+ flow cytometry (Hansen et al., 2018; Kattman et al., 2011; Lundy, Zhu, Regnier, & Laflamme, 2013a). hiPS-CMs were thawed and seeded in RPMI-B27 media, 10% fetal bovine serum (FBS; Gibco), and 1% Rho-associated protein kinase (ROCK) inhibitor (Y-27632 dihydrochloride, Sigma Aldrich) to reduce cell apoptosis. hiPS-CMs were seeded on leaves in 10 mm diameter cloning wells at 150,000–200,000 cells per leaf (191,000–255,000 cells/cm^2) and incubated for 18 hours at 37°C. As positive controls, 156,250 hiPS-CMs/cm^2 were seeded on ECM coated and noncoated tissue culture plastic (TCP). Cells were cultured in RPMI-B27 media on leaves and controls at 37°C for 7, 14, and 21 days ($N = 3$ biological replicates). RPMI-B27 cell media was replenished every 2–3 days. Samples were fixed in 4% paraformaldehyde (PFA) at days 7, 14, and 21.

2.4 | Effect of FBS on hiPS-CM adhesion to decellularized leaves

To determine if initial hiPS-CM seeding with FBS had an effect on cell binding to leaves, we seeded hiPS-CMs on noncoated decellularized spinach leaves, as previously detailed, with or without FBS. hiPS-CM FBS seeding media contained RPMI-B27, 10% FBS (Gibco), and 1% ROCK inhibitor (Y-27632 dihydrochloride, Sigma Aldrich). hiPS-CM seeding media without FBS was composed of RPMI-B27 and 1% ROCK inhibitor (Y-27632 dihydrochloride, Sigma Aldrich). hiPS-CMs were incubated with or without FBS on leaves ($n = 6$) for 18 hours at 37°C. RPMI-B27 media was replenished after 18 hours, and then every 2 days. Samples were fixed in 4% PFA after 7 days in culture.

2.5 | hiPS-CM contractile function

Cardiac left ventricular contraction is defined by tissue deformation and strain in the left ventricle in vivo (Arts & Reneman, 1980). Measuring strain in contracting hiPS-CMs can be accomplished optically and noninvasively under a microscope with a high-speed camera (Czirok et al., 2017; Gaudette, Todaro, Azeloglu, Krukenkamp, & Chiang, 2002; Kamgoué, Ohayon, Usson, Riou, & Tracqui, 2009; Kelly, Azeloglu, Kochupura, Sharma, & Gaudette, 2007). We used high density mapping (HDM), as previously described (Hansen et al., 2017; Kelly et al., 2007), to measure hiPS-CM contractile strain on decellularized spinach leaves. Live hiPS-CM contraction videos were visualized with an inverted microscope (DMIL, Leica Microsystems, Buffalo Grove, IL) and recorded at 60 frames per second with a high-speed camera (HiSpec 4, Fastec Imaging Corp, San Diego, CA). HDM analysis of hiPS-CM contraction was performed using code written in MATLAB (MathWorks, Natick, MA), previously explained in detail (Hansen et al., 2017). Contractile strain measurements of

hiPS-CMs on coated and noncoated leaf samples and TCP were collected at one time point, either Day 7, 14, or 21. Cardiomyocyte contractions on leaves was visualized over time (Figure 1). Video data from one to five regions on a sample was analyzed, based on number of observed hiPS-CM contractile areas on a sample. Contractile strain was reported as the maximum contractile principle strain value from initiation of contraction in a determined cell region (Hansen et al., 2017), and sample contractile strain was defined as the mean ± standard deviation of the regions. Immediately after data collection, samples were fixed in 4% PFA and stored in 1X PBS at 4°C.

2.6 | Immunofluorescence image analysis

hiPS-CM seeded decellularized spinach leaf scaffolds were immunolabeled for sarcomeric α-actinin (mouse or rabbit, Abcam) and connexin-43 (goat, Abcam) primary antibodies to indicate cell adhesion, spreading, sarcomere length and gap junctions. Secondary antibodies Alexa Fluor 488 (Invitrogen) or Alexa Fluor 647 (Invitrogen) were used for sarcomeric α-actinin. Connexin-43 was immunolabeled with Alexa Fluor 568 (Invitrogen) secondary antibody. hiPS-CM nuclei were indicated with Hoescht 33342 nuclear stain (Life Technologies). Antibody host species, vendors, and dilution factors are specified in Figure S1. Samples were imaged with a scanning confocal microscope (Leica Microsystems, Buffalo Grove, IL).

2.7 | hiPS-CM sarcomeric length on leaf scaffolds

Cardiomyocyte sarcomere length is indicative of cell behavior since length is associated with cardiac muscle contraction mechanics and cell maturity (Lundy, Zhu, Regnier, & Laflamme, 2013b; Rodriguez et al., 2014). hiPS-CM sarcomere length was calculated by measuring the distance between Z-disks, indicated by positive immunofluorescence (IF) sarcomeric α-actinin images, using Fourier transform analysis (Figure 2). Sarcomere length was analyzed in ImageJ (NIH) and MATLAB (MathWorks, Natick, MA). A collected IF image was opened in ImageJ and a random array of visible cell sarcomeres was selected in an α-actinin positive cell. A line was drawn perpendicular to the sarcomere bands, and the grey value peaks were plotted in ImageJ using the “Plot Profile” function (Figure 2a,b). Discrete Fourier transforms and power spectrum analysis of the sarcomere grey values were performed in MATLAB (Figure 2c,d), calculating the cell’s sarcomere length. Sarcomere band data between one and 18 cells on a leaf sample were collected and the sample sarcomere length was defined as the mean ± standard deviation.

2.8 | hiPS-CM spreading on leaf scaffolds

hiPS-CM cell spreading and sarcomeric striation is an indication of cell adherence and eventual maturation (Lundy et al., 2013b). hiPS-CMs were indicated with positive sarcomeric α-actinin staining. Cells were deemed spreading if hiPS-CM sarcomeres extended beyond the circumference of the cell nucleus. Data were collected from between two and six regions on a leaf sample and cell spreading was defined as the mean ± standard deviation. Data is presented as the percent of elongated hiPS-CMs out of the total hiPS-CM population per mm^2 of leaf surface. Total cell number is the mean number of cells in a sample per mm^2 of leaf surface, or density.

2.9 | Statistical analysis

This study analyzed $N = 3$ biological replicates for each time and coating condition. All results are presented as mean ± standard deviation. Statistical significance between ECM coatings was tested with one-way ANOVA and post-hoc Tukey t-tests ($p < .05$). Statistical significance between hiPS-CM contractile strain on noncoated leaves with or without FBS in seeding media was tested with an unpaired t test ($p < .05$). All statistical analyses were performed in GraphPad Prism 8 (GraphPad Software, San Diego, CA).

3 | RESULTS

Spinach leaves were decellularized, sterilized, and coated with either fibronectin or collagen IV ECM protein. Immunofluorescence staining demonstrated that both ECM protein coatings adhered to the surface of decellularized spinach leaves (Figure S2). Furthermore, hiPS-CMs adhered to decellularized spinach leaves with and without ECM coatings for 21 days (Figure 3), indicating that ECM protein coatings are uneccessary for hiPS-CM adherence on leaves.

To study if FBS had an effect on cell adherence to noncoated decellularized spinach leaves, we removed FBS from hiPS-CM seeding media. After 7 days in culture on leaves, hiPS-CMs remained adherent to noncoated leaves with and without FBS at initial cell seeding. Both seeding conditions had variable cell morphologies on leaf scaffolds, illustrating both elongated sarcomeric bands and round cell clusters. In addition, there were no statistically significant differences in hiPS-CM maximum contractile strain with or without FBS ($p = .22$) (Figure S3).

3.1 | Contractile strain analysis

hiPS-CMs contracted on spinach leaves at all time points and under all coating conditions (Figure 4a); however, we did not always observe hiPS-CM contractile behavior with live video imaging. Contractile strain was analyzed in n ≥ 4 samples per condition and time point. We only observed contraction for $N = 2$ of 3 biological replicates of hiPS-CMs on collagen IV coated leaves at Day 14 and on fibronectin TCP at Day 21. All maximum contractile strains were larger than 1.5%. No statistically significant differences in maximum contractile strain between hiPS-CMs seeded on coated and noncoated leaves and TCP at each time point nor over time were observed (Figure 4a,b). There were no significant differences in maximum contractile strain of hiPS-CMs on ECM coated and noncoated leaves at days 7 and 21. However, strain on collagen IV coated leaves (3.25 ± 0.39%) were significantly larger than noncoated leaves (1.54 ± 0.60%) ($p = .03$) at Day 14. This observation was the only significant difference for all leaf coatings and time points. No differences in hiPS-CM contractile strain were found between these samples and corresponding collagen IV coated TCP (2.65 ± 0.97%) or noncoated TCP (2.11 ± 0.48%) at Day 14.

3.2 | Sarcomere length

Sarcomere length was determined in n ≥ 4 samples per condition. Average hiPS-CM sarcomere lengths ranged from 1.65 ± 0.18 μm on collagen IV coated leaves at Day 7 to 2.06

± 0.06 μm on fibronectin coated leaves at Day 14. There was no statistically significant differences in hiPS-CM sarcomere length between leaf coatings at Day 7 and 21 (Figure 5a). In addition, there was no significant differences in collagen IV coated and noncoated leaf samples over time. There was a statistically significant increase in hiPS-CM sarcomere length on fibronectin coated leaves at Day 14 compared to Day 7 ($p = .008$) and Day 21 ($p = .04$). In addition, sarcomeres on fibronectin coated leaves were statistically longer than on collagen IV coated leaves at Day 14 ($p = .006$).

3.3 | Cell spreading

hiPS-CM cell count and spreading was calculated with n ≥ 8 samples for each leaf condition. We observed cell spreading and elongation in more than 37% of hiPS-CMs on ECM coated and noncoated leaves, observed by IF imaging. There was no significant differences in spreading between leaf coatings and time points (Figure 5b). However, at Day 14, we observed decreased average sample cell density compared to Day 7 (not significant) and Day 21 ($p = .03$) on fibronectin coated leaves (Figure 6). At Day 14, fibronectin coated leaves also had decreased cell spreading compared to Day 7 and 21 (not significant).

4 | DISCUSSION

The major limitation affecting current tissue engineered solutions is the lack of adequate vasculature. As tissue thickness increases, vasculature is needed to properly provide oxygen and nutrients to all parts of the tissue. Thick engineered cardiac tissue for implantation requires a vasculature to provide nutrients and remove waste to retain tissue viability because cells are only able to survive a maximum of 200 μm from a nutrient source due to limitations of oxygen diffusion (Mao & Mooney, 2015; Riemenschneider et al., 2016). Ideally, the vasculature of engineered tissues must be integrated, branched and perfusable to maintain tissue function. Lack of vasculature limits the thickness of current scaffolds, reducing clinical efficacy and limiting use in humans. Few engineered constructs demonstrate immediate functional vascular flow through engineered tissues in vitro and in vivo, and have delayed integration and neovascularization after in vivo implantation (Coulombe & Murry, 2014; Kreutziger et al., 2011; Masumoto et al., 2015; Novosel, Kleinhans, & Kluger, 2011).

Inspired by nature, we found leaves have many desirable properties for cardiac tissue engineering. Leaves have a native vasculature with branching similar to that of the human cardiovascular system (McCulloh et al., 2003). Previous work showed that we can decellularize spinach leaves and their vascular system remains patent. Furthermore, we showed that we can coat the leaf vasculature with human umbilical vein endothelial cells, mimicking the inner lining of mammalian blood vessels (Gershlak et al., 2017). This work demonstrates a possible novel tissue engineered cardiac patch with an inherent mature vascular system.

Decellularized leaves are primarily composed of cellulose, a biocompatible biomaterial commonly used in tissue engineering. Cellulose is used in other fields of tissue engineering research and in FDA-approved surgical hemostatic wound dressings (Entcheva et al., 2004; Hart et al., 2002; Helenius et al., 2006; Modulevsky et al., 2016). Cellulose scaffolds

modified with ECM proteins before cell seeding have been found to change cell behavior. For example, seeding C2C12 mouse myoblasts in type I collagen hydrogels increased cell adhesion on plant-derived cellulose (Hickey, Modulevsky, Cuerrier, & Pelling, 2018). For cardiac tissue engineering application, fibronectin coated cellulose polymer scaffolds promote maturation of neonatal cardiac myocytes by sarcomere organization and increased gap junction density (Entcheva et al., 2004). In addition, hiPS-CMs have been found to contract, electrically couple with host cardiomyocytes (Eschenhagen et al., 2017) and improve function with the attenuation of ventricle remodeling after MI in vivo (Masumoto et al., 2015; Wendel et al., 2015). This can be explained by the observation that cardiomyocytes bind to ECM with cell integrin receptors and form focal adhesions to the matrix (Stevens & George, 2005; Wu et al., 2010), which in turn can influence cardiomyocyte behavior and maturation (Baharvand, Azarnia, Parivar, & Ashtiani, 2005). Our previous studies coated decellularized spinach leaves with ECM proteins found in adult heart (Gershlak et al., 2017). We were interested in removing the ECM coating from the leaf scaffold while retaining similar cell behavior on the scaffold. Herein, we determined that ECM coatings are not necessary for hiPS-CM adherence and function on decellularized leaves. We hypothesize that cells bind to noncoated decellularized leaves due to the scaffold's cellulose composition. Cellulose's polysaccharide structure may positively interact with the cell surface glycocalyx (Entcheva et al., 2004), reducing the need for ECM coatings on the scaffold's surface. FBS proteins, present during hiPS-CM seeding, may bind directly to noncoated leaves and provide a substrate for cell adhesion; however, including FBS is not necessary for hiPS-CM adhesion or contraction on the leaf scaffold. We observed that hiPS-CMs adhere to noncoated decellularized spinach leaves with and without FBS in the seeding media. Furthermore, we found no functional significant differences in contractile behavior between the two seeding conditions after 7 days, indicating that FBS is not necessary to culture contractile hiPS-CMs on leaves.

Eliminating the ECM coating step has several advantages in creating a tissue engineered cardiac patch for implantation. First, the preparation time and steps to manufacture the tissue would be reduced, which therefore decreases manufacturing complexity. This would eliminate additional contamination risks during manufacturing and increase speed of manufacturing. Faster manufacturing could then lead to decreased production and product costs. Furthermore, including ECM coatings on the tissue would add an additional concern for FDA approval. The sources of the ECM would have to be controlled and qualified, increasing time and cost of approval. Removal of the ECM would eliminate this testing and allow for a faster regulatory approval process.

When evaluating novel scaffolds for cardiac tissue engineering, it is important to consider tissue deformation, or contractile strain, which is indicative of left ventricular function. In this study, we found no statistically significant differences in contractile strain between hiPS-CMs seeded on ECM coated and noncoated leaves and TCP over 21 days. In addition, contractile strains were not significantly different from the TCP controls. We also observed a trend toward decreased contractile strain from Day 7 to 14 for all conditions, although this did not reach statistical significance. This corresponded with decreased cell spreading (not significant) and cell number (not significant) from Day 7 to 14. The decreasing trend could be related to the drastic difference between the substrate stiffnesseses of leaves and TCP. We

previously determined that the maximum tangent modulus for decellularized spinach leaves is 0.3 MPa (Gershlak et al., 2017), within the range of adult human myocardium (10–500 kPa) (Huyer, Montgomery, Zhao, et al., 2015). Whereas, polystyrene plastic has an elastic modulus of 3 GPa (Gilbert, Havenstrite, Magnusson, et al., 2010), three orders of magnitude larger. Neonatal cardiomyocytes cultured on stiff substrates have been found to have less sarcomere definition and alignment than those cultured on substrates with stiffnesses similar to native myocardium. This can interrupt cardiomyocyte maturation, decrease contractile forces, and cardiomyocytes can form actin stress fibers as they mature (Jacot, McCulloch, & Omens, 2008). We hypothesize that decreased hiPS-CM cell contractility observed at Day 14, specifically in TCP culture, may be due to its stiff surface substrate. With long-term culture on TCP, differences in hiPS-CM contractile and morphology behavior could become more evident over time.

This study observed larger cardiomyocyte contractile strain values on decellularized spinach leaves than previous findings (Gershlak et al., 2017). Previous contractile strain analysis determined hPS-CM strain to be 0.6% on fibronectin coated decellularized spinach leaves at Day 21. Our findings demonstrate 3.94 ± 1.20% contractile strain on fibronectin coated leaves at Day 21. This could be due to recent changes in decellularization techniques. We found that using 1% SDS is as effective as 10% SDS to decellularize spinach leaves. Higher SDS concentrations may affect leaf substrate stiffness and reduce the contractility of adherent cardiomyocytes. Although cardiomyocyte contractility increased, hiPS-CMs' contractile strains on decellularized leaves were still less than the human myocardium (15.9–22.1%) (Yingchoncharoen, Agarwal, Popovic, & Marwick, 2013). This is likely due to several factors. Strain depends on cardiomyocyte orientation. Aligned hiPS-CMs show improved contractile performance versus nonaligned hiPS-CMs (Ribeiro et al., 2015). This study focused on the ability for decellularized leaves to support hiPS-CM function with and without ECM surface coatings. In future work, we will focus on improving contractility of the seeded hiPS-CMs with cell alignment. Another factor to contribute to differences in strain magnitudes is the thickness of the cell layer. The scaffolds presented here are monolayers, whereas human myocardium is hundreds of cell layers thick. These extra cells help deform the substrate, resulting in increased contractile strain.

Variability in strain measurements or average cell number could also be explained, in part, by exposure to room temperature conditions during data acquisition. Image-based strain data collection is performed at room temperature and can take as long as 10 minutes per sample. Samples were cultured in multi-well plates and therefore, contractile samples could have been exposed to room temperature for longer than 10 minutes. To minimize the effects of temperature, plates were returned to the 37°C incubator after data collection of three samples for at least 15 minutes before continuing with data collection. Furthermore, this study used unpaired samples to avoid performing repeated data collection, potentially affecting strain results over time. Future studies may consider returning multiwell plates to the incubator after one sample data collection to minimize any temperature effects on strain data or cell number.

hiPS-CMs contain a mixed cell population of atrial, ventricular and nodal cardiomyocytes after cardiac differentiation (Shiba, Hauch, & Laflamme, 2010; Zhang, Wilson, Soerens, et

al., 2009). Nodal cells propogate action potentials, stimulating cardiomyocyte contraction. We found that a majority of hiPS-CMs on leaves contracted. However, some sarcomeric α-actinin positive samples were not contractile during strain data collection. This explains the different sample sizes of measured strain compared to IF image analysis. For example, there were less contractile hiPS-CM samples on collagen IV coated leaf scaffolds at Day 14 (N = 2, n = 4) for strain analysis than sarcomeric α-actinin positive samples for sarcomere length analysis (N = 3, n = 8).

Culture time is linked to increased sarcomere length and maturation. IF cell spreading data indicated no significant differences in spreading and maturity between leaf coatings. Furthermore, sarcomere lengths of hiPS-CMs on leaves were comparable to previous findings. Resting sarcomere length of human embryonic stem cell-derived cardiomyocytes (hES-CMs) in culture dishes has been found to increase from an average of 1.65 μm in early-stage hES-CMs to 1.81 μm ($p < .001$) in late-stage hES-CMs (Lundy et al., 2013b). hiPS-CM sarcomere lengths on noncoated decellularized spinach leaves were similar to or exceeded these findings. Average sarcomere lengths of hiPS-CMs cultured on noncoated decellularized leaf scaffolds for 21 days ranged from 1.80 ± 0.05 μm to 1.84 ± 0.14 μm, comparable to late-stage hES-CMs in culture dishes. Overall, average hiPS-CM sarcomere length on leaves approaches average sarcomere length of adult cardiomyocytes (1.8 μm to 2.2 μm).

Too much of an increase in sarcomere length (above 2.2 μm) is associated with the pathophysiology of heart disease and heart failure since chronic dilation in the diseased ventricle results in increased cardiomyocyte lengths. This length increase is associated with loss of function by decreased cardiac contractility, according to the Frank–Starling mechanism (Opie, Commerford, Gersh, & Pfeffer, 2006; Sahli Costabal et al., 2019). We did not observe hiPS-CM sarcomere lengths larger than 2.2 μm on coated or noncoated decellularized spinach leaves. Furthermore, we did not observe increases in hiPS-CM sarcomere length and decreased contractile strain values on non-coated leaves, which corresponds to the pathophysiology of heart failure.

5 | CONCLUSIONS

This study is the first to demonstrate the development of a plant-based, cardiomyocyte containing, contractile biomaterial without the use of ECM protein coatings. When seededed with hiPS-CMs, non-coated decellularized leaves have comparable hiPS-CM contractile function as fibronectin and collagen IV coated leaves. ECM protein coatings are not necessary to improve cardiomyocyte cell adhesion, behavior, and contractility on decellularized leaf scaffolds. Decellularized spinach leaves can serve as inexpensive, abundant, and sustainable pre-vascularized scaffolds for cardiac tissue engineering. Noncoated decellularized leaf surfaces allow for simple cell attachment for an engineered tissue patch, and we are able to provide the appropriate environment for hiPS-CMs to adhere. The decellularized leaf holds significant potential as a scaffold for a cardiac tissue engineered patch to refunctionalize diseased cardiac tissue. The decellularized leaf merits further investigation as a scaffold for a tissue engineered patch to refunctionalize diseased cardiac tissue.

Supplementary Material

Refer to Web version on PubMed Central for supplementary material.

ACKNOWLEDGMENT

Joshua R. Gershlak for spinach leaf decellularization technique. This study was supported by National Institutes of Health grants R01-HL115282 (G.R.G.) and R15-HL137145 (G.D.P).

Funding information

National Institutes of Health, Grant/Award Numbers: R15-HL137145, RO1-HL115282

REFERENCES

Arts T, & Reneman RS (1980). Measurement of deformation of canine epicardium in vivo during cardiac cycle. American Journal of Physiology-Heart and Circulatory Physiology, 239(8), H432–H437. http://www.ncbi.nlm.nih.gov/pubmed/7435589

Baharvand H, Azarnia M, Parivar K, & Ashtiani SK (2005). The effect of extracellular matrix on embryonic stem cell-derived cardiomyocytes. Journal of Molecular and Cellular Cardiology, 38(3), 495–503. 10.1016/j.yjmcc.2004.12.011 [PubMed: 15733909]

Benjamin EJ, Blaha MJ, Chiuve SE, & Cushman M (2017). Heart disease and stroke statistics—2017 update. Circulation, 135(10), e146–e603. 10.1161/CIR.0000000000000485.Heart [PubMed: 28122885]

Colvin M, Smith JM, Skeans MA, Edwards LB, Uccellini K, Snyder JJ, … Kasiske BL (2017). OPTN/SRTR 2015 annual data report: Heart. American Journal of Transplantation, 17(Suppl 1), 286–356. 10.1111/ajt.14128 [PubMed: 28052610]

Coulombe KLK, & Murry CE (2014). Vascular perfusion of implanted human engineered cardiac tissue. Proceeding IEEE Annual Northeast Bioengineering Conference, 2014, 1–7. 10.1007/s00210-015-1172-8.The

Czaja WK, Young DJ, Kawecki M, & Brown RM (2007). The future prospects of microbial cellulose in biomedical applications. Biomacromolecules, 8(1), 1–12. 10.1021/bm060620d [PubMed: 17206781]

Czirok A, Isai DG, Kosa E, Rajasingh S, Kinsey W, Neufeld Z, & Rajasingh J (2017). Optical-flow based non-invasive analysis of cardiomyocyte contractility. Scientific Reports, 7(1), 1–11. 10.1038/s41598-017-10094-7 [PubMed: 28127051]

Entcheva E, Bien H, Yin L, Chung CY, Farrell M, & Kostov Y (2004). Functional cardiac cell constructs on cellulose-based scaffolding. Biomaterials, 25(26), 5753–5762. 10.1016/j.biomaterials.2004.01.024 [PubMed: 15147821]

Eschenhagen T, Bolli R, Braun T, Field LJ, Fleischmann BK, Frisén J, … Hill JA (2017). Cardiomyocyte regeneration: A consensus statement. Circulation, 136, 1–8. 10.1161/CIRCULATIONAHA.117.029343

Gaudette GR, Todaro J, Azeloglu EU, Krukenkamp IB, & Chiang F-P (2002). Determination of regional stroke work with high spatial resolution in the isolated beating rabbit heart. Cardiovascular Engineering, 2(4), 129–137.

Gershlak JR, Hernandez S, Fontana G, Perreault LR, Hansen KJ, Larson SA, … Gaudette GR (2017). Crossing kingdoms: Using decellularized plants as perfusable tissue engineering scaffolds. Biomaterials, 125, 13–22. 10.1016/j.biomaterials.2017.02.011 [PubMed: 28222326]

Gilbert PM, Havenstrite KL, Magnusson KEG, Sacco A, Leonardi NA, Kraft P, … Blau HM (2010). Substrate elasticity regulates skeletal muscle stem cell self-renewal in culture. Science, 329(5995), 1078–1081. 10.1126/science.1191035 [PubMed: 20647425]

Guyette JP, Charest JM, Mills RW, Jank BJ, Moser PT, Gilpin SE, … Ott HC (2016). Bioengineering human myocardium on native extracellular matrix. Circulation Research, 118(1), 56–72. 10.1161/CIRCRESAHA.115.306874 [PubMed: 26503464]

Guyette JP, Gilpin SE, Charest JM, Tapias LF, Ren X, & Ott HC (2014). Perfusion decellularization of whole organs. Nature Protocols, 9 (6), 1451–1468. 10.1038/nprot.2014.097 [PubMed: 24874812]

Hansen KJ, Favreau JT, Gershlak JR, Laflamme MA, Albrecht DR, & Gaudette GR (2017). Optical method to quantify mechanical contraction and calcium transients of human pluripotent stem cell-derived Cardiomyocytes. Tissue Engineering. Part C, Methods, 23(8), 445–454. 10.1089/ten.tec.2017.0190 [PubMed: 28562232]

Hansen KJ, Laflamme MA, & Gaudette GR (2018). Development of a contractile cardiac fiber from pluripotent stem cell derived Cardiomyocytes. Frontiers in Cardiovascular Medicine, 5(52), 1–11. 10.3389/fcvm.2018.00052 [PubMed: 29404341]

Hart J, Silcock D, Gunnigle S, Cullen B, Light ND, & Watt PW (2002). The role of oxidised regenerated cellulose/collagen in wound repair: Effects in vitro on fibroblast biology and in vivo in a model of compromised healing. The International Journal of Biochemistry & Cell Biology, 34(12), 1557–1570. 10.1016/S1357-2725(02)00062-6 [PubMed: 12379278]

Helenius G, Bäckdahl H, Bodin A, Nannmark U, Gatenholm P, & Risberg B (2006). In vivo biocompatibility of bacterial cellulose. Journal of Biomedical Materials Research - Part A., 76(2), 431–438. 10.1002/jbm.a.30570 [PubMed: 16278860]

Hickey RJ, Modulevsky DJ, Cuerrier CM, & Pelling AE (2018). Customizing the shape and microenvironment biochemistry of bio-compatible macroscopic plant-derived cellulose scaffolds. ACS Biomaterials Science & Engineering, 4, 3726–3736. 10.1021/acsbiomaterials.8b00178

Huyer LD, Montgomery M, Zhao Y, Xiao Y, Conant G, Korolj A, & Radisic M (2015). Biomaterial based cardiac tissue engineering and its applications. Biomedical Materials, 10(3). 10.1088/1748-6041/10/3/034004

Jacot JG, McCulloch AD, & Omens JH (2008). Substrate stiffness affects the functional maturation of neonatal rat ventricular myocytes. Biophysical Journal, 95(7), 3479–3487. 10.1529/biophysj.107.124545 [PubMed: 18586852]

Kamgoué A, Ohayon J, Usson Y, Riou L, & Tracqui P (2009). Quantification of cardiomyocyte contraction based on image correlation analysis. Cytom Part A., 75A, 298–308. 10.1002/cyto.a.20700

Kattman SJ, Witty AD, Gagliardi M, Dubois NC, Niapour M, Hotta A, … Keller G (2011). Stage-specific optimization of activin/nodal and BMP signaling promotes cardiac differentiation of mouse and human pluripotent stem cell lines. Cell Stem Cell, 8(2), 228–240. 10.1016/j.stem.2010.12.008 [PubMed: 21295278]

Kelly DJ, Azeloglu EU, Kochupura PV, Sharma GS, & Gaudette GR (2007). Accuracy and reproducibility of a subpixel extended phase correlation method to determine micron level displacements in the heart. Medical Engineering & Physics, 29(1), 154–162. 10.1016/j.medengphy.2006.01.001 [PubMed: 16531092]

Kreutziger KL, Muskheli V, Johnson P, Braun K, Wight TN, & Murry CE (2011). Developing vasculature and Stroma in engineered human myocardium. Tissue Engineering. Part A, 17(9–10), 1219–1228. 10.1089/ten.tea.2010.0557 [PubMed: 21187004]

Lundy SD, Zhu W-Z, Regnier M, & Laflamme MA (2013a). Structural and functional maturation of Cardiomyocytes derived from human pluripotent stem cells. Stem Cells and Development, 22(14), 1991–2002. 10.1089/scd.2012.0490 [PubMed: 23461462]

Mao AS, & Mooney DJ (2015). Regenerative medicine: Current therapies and future directions. Proceedings of the National Academy of Sciences, 112(47), 14452–14459. 10.1073/pnas.1508520112

Masumoto H, Ikuno T, Takeda M, Fukushima H, Marui A, Katayama S, … Yamashita JK (2015). Human iPS cell-engineered cardiac tissue sheets with cardiomyocytes and vascular cells for cardiac regeneration. Scientific Reports, 4(1), 6716 10.1038/srep06716

Matsuda K, Falkenberg KJ, Woods AA, Choi YS, Morrison WA, & Dilley RJ (2013). Adipose-derived stem cells promote angiogenesis and tissue formation for in vivo tissue engineering. Tissue Engineering. Part A, 19(11–12), 1327–1335. 10.1089/ten.TEA.2012.0391 [PubMed: 23394225]

McCulloh KA, Sperry JS, & Adler FR (2003). Water transport in plants obeys Murray's law. Nature, 421(February), 939–942. 10.1038/nature01438.1 [PubMed: 12607000]

Modulevsky DJ, Cuerrier CM, & Pelling AE (2016). Biocompatibility of subcutaneously implanted plant-derived cellulose biomaterials. PLoS One, 11(6), 1–19. 10.1371/journal.pone.0157894

Novosel EC, Kleinhans C, & Kluger PJ (2011). Vascularization is the key challenge in tissue engineering. Advanced Drug Delivery Reviews, 63(4), 300–311. 10.1016/j.addr.2011.03.004 [PubMed: 21396416]

Opie LH, Commerford PJ, Gersh BJ, & Pfeffer M (2006). A, England N. controversies in ventricular remodelling. Lancet, 367(9507), 356–367. [PubMed: 16443044]

Ott HC, Matthiesen TS, Goh S-K, Black LD, Kren SM, Netoff TI, & Taylor DA (2008). Perfusion-decellularized matrix: Using nature's platform to engineer a bioartificial heart. Nature Medicine, 14(2), 213–221. 10.1038/nm1684

Parsa H, Ronaldson K, & Vunjak-Novakovic G (2016). Bioengineering methods for myocardial regeneration. Advanced Drug Delivery Reviews, 96, 195–202. 10.1016/j.addr.2015.06.012 [PubMed: 26150344]

Ribeiro AJS, Ang Y-S, Fu J-D, Rivas RN, Mohamed TMA, Higgs GC, … Pruitt BL (2015). Contractility of single cardiomyocytes differentiated from pluripotent stem cells depends on physiological shape and substrate stiffness. Proceedings of the National Academy of Sciences, 112(41), 12705–12710. 10.1073/pnas.1508073112

Riemenschneider SB, Mattia DJ, Wendel JS, Schaefer JA, Ye L, Guzman PA, & Tranquillo RT (2016). Inosculation and perfusion of pre-vascularized tissue patches containing aligned human microvessels after myocardial infarction. Biomaterials, 97, 51–61. 10.5588/ijtld.16.0716.Isoniazid [PubMed: 27162074]

Rodness J, Mihic A, Miyagi Y, Wu J, Weisel RD, & Li RK (2016). VEGF-loaded microsphere patch for local protein delivery to the ischemic heart. Acta Biomaterialia, 45, 169–181. 10.1016/j.actbio.2016.09.009 [PubMed: 27619839]

Rodriguez ML, Graham BT, Pabon LM, Han SJ, Murry CE, & Sniadecki NJ (2014). Measuring the contractile forces of human induced pluripotent stem cell-derived Cardiomyocytes with arrays of microposts. Journal of Biomechanical Engineering, 136(5), 051005 10.1115/1.4027145 [PubMed: 24615475]

Sahli Costabal F, Choy JS, Sack KL, Guccione JM, Kassab GS, & Kuhl E (2019). Multiscale characterization of heart failure. Acta Biomaterialia, 86, 66–76. 10.1016/j.actbio.2018.12.053 [PubMed: 30630123]

Schwan J, Kwaczala AT, Ryan TJ, Bartulos O, Ren Y, Sewanan LR, … Campbell SG (2016). Anisotropic engineered heart tissue made from laser-cut decellularized myocardium. Scientific Reports, 6, 1–12. 10.1038/srep32068 [PubMed: 28442746]

Shevach M, Soffer-Tsur N, Fleischer S, Shapira A, & Dvir T (2014). Fabrication of omentum-based matrix for engineering vascularized cardiac tissues. Biofabrication, 6(2), 024101 10.1088/1758-5082/6/2/024101 [PubMed: 24464690]

Shiba Y, Hauch KD, & Laflamme MA (2010). Cardiac applications for human pluripotent stem cells. Current Pharmaceutical Design, 46 (2), 220–231. 10.1016/j.freeradbiomed.2008.10.025.The

Song JJ, & Ott HC (2011). Organ engineering based on decellularized matrix scaffolds. Trends in Molecular Medicine, 17(8), 424–432. 10.1016/j.molmed.2011.03.005 [PubMed: 21514224]

Stevens MM, George JH. Exploring and engineering the cell surface Interface. Science (80-). 2005;310:1135–1138. 10.1126/science.1106587

Takahashi K, & Yamanaka S (2006). Induction of pluripotent stem cells from mouse embryonic and adult fibroblast cultures by defined factors. Cell, 126(4), 663–676. 10.1016/j.cell.2006.07.024 [PubMed: 16904174]

Wendel JS, Ye L, Tao R, Zhang J, Zhang J, Kamp TJ, & Tranquillo RT (2015). Functional effects of a tissue-engineered cardiac patch from human induced pluripotent stem cell-derived Cardiomyocytes in a rat infarct model. Stem Cells Translational Medicine, 4(11), 1324–1332. 10.5966/sctm.2015-0044 [PubMed: 26371342]

Williams C, Quinn KP, Georgakoudi I, & Black LD (2014). Young developmental age cardiac extracellular matrix promotes the expansion of neonatal cardiomyocytes in vitro. Acta Biomaterialia, 10(1), 194–204. 10.1016/j.actbio.2013.08.037 [PubMed: 24012606]

Wu X, Sun Z, Foskett A, Trzeciakowski JP, Meininger GA, & Muthuchamy M (2010). Cardiomyocyte contractile status is associated with differences in fibronectin and integrin interactions. American Journal of Physiology. Heart and Circulatory Physiology, 298(6), H2071–H2081. 10.1152/ajpheart.01156.2009 [PubMed: 20382852]

Yancy CW, Jessup M, Bozkurt B, Butler J, Casey DE Jr., Drazner MH, … American College of Cardiology Foundation, American Heart Association Task Force on Practice Guidelines. (2013). 2013 ACCF/AHA guideline for the management of heart failure: A report of the American college of cardiology foundation/american heart association task force on practice guidelines. Journal of the American College of Cardiology, 62(16), e147–e239. 10.1016/j.jacc.2013.05.019 [PubMed: 23747642]

Yang L, Soonpaa MH, Adler ED, Roepke TK, Kattman SJ, Kennedy M, … Keller GM (2008). Human cardiovascular progenitor cells develop from a KDR+ embryonic-stem-cell-derived population. Nature, 453(7194), 524–528. 10.1038/nature06894 [PubMed: 18432194]

Yingchoncharoen T, Agarwal S, Popovic Z, & Marwick T (2013). Normal ranges of left ventricular strain: A meta-analysis. Journal of the American Society of Echocardiography, 26(2), 185–191. [PubMed: 23218891]

Yu J, Smuga-Otto K, Vodyanik M. a, Antosiewicz-Bourget J, Frane JL, Tian S, … Thomson JA (2007). Induced pluripotent stem cell lines derived from human somatic cells. Science, 318(5858), 1917–1920. 10.1126/science.1151526 [PubMed: 18029452]

Zhang J, Wilson GF, Soerens AG, Koonce CH, Yu J, Palecek SP, … Kamp TJ (2009). Functional cardiomyocytes derived from human induced pluripotent stem cells. Circulation Research, 104(4), e30–e41. 10.1161/CIRCRESAHA.108.192237 [PubMed: 19213953]

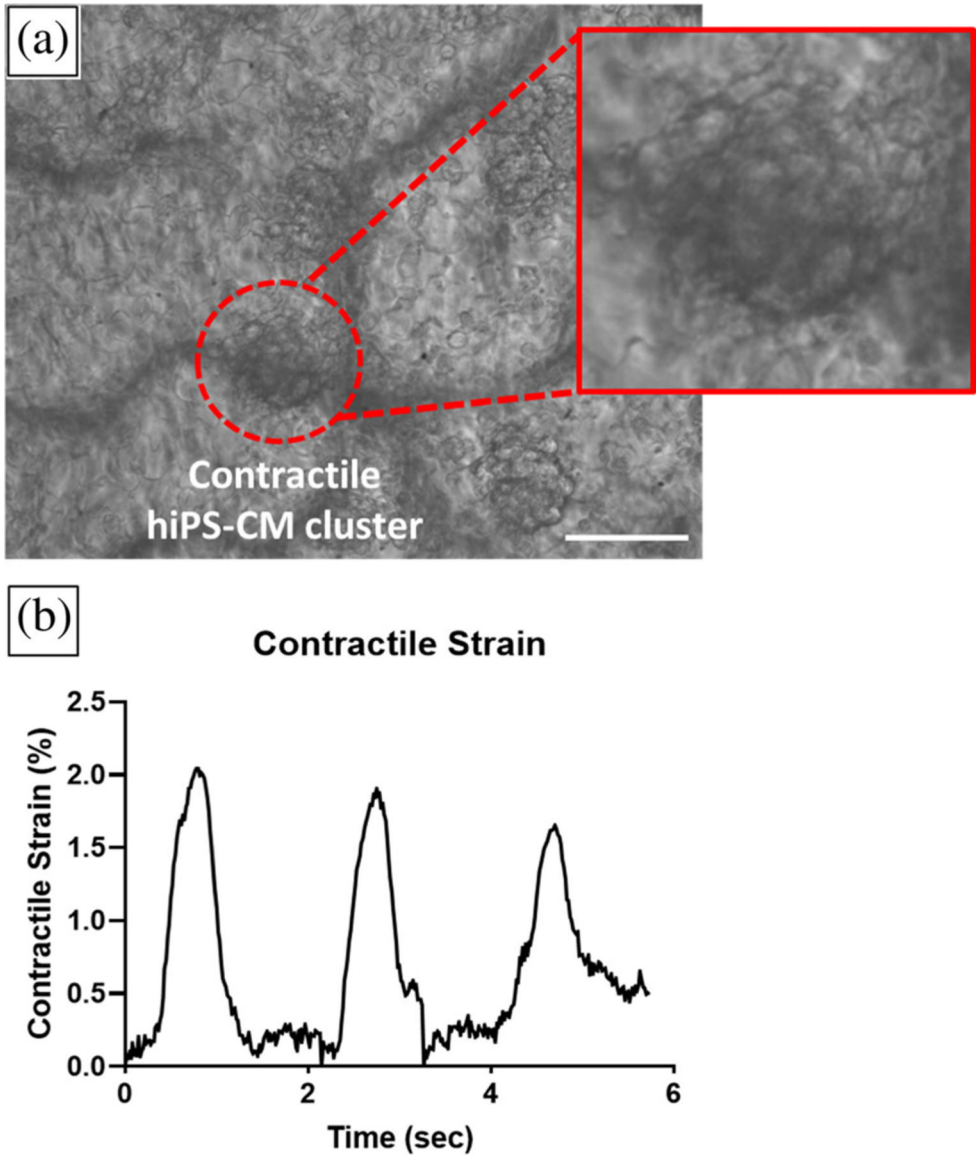

FIGURE 1.

High density mapping analysis of hiPS-CM contractile strain on a noncoated decellularized spinach leaf. (a) Single frame of high speed contraction video of hiPS-CMs on a noncoated decellularized spinach leaf. High density mapping (HDM) strain analysis was performed on contractile hiPS-CM clusters on decellularized leaves, illustrated in red circle. The inset visualizes several cells on the leaf. Scale bar 50 μm. (b) Contractile strain of the hiPS-CM cluster was measured with HDM over time. Peaks in strain plot indicate maximum strain per contraction on the leaf's surface

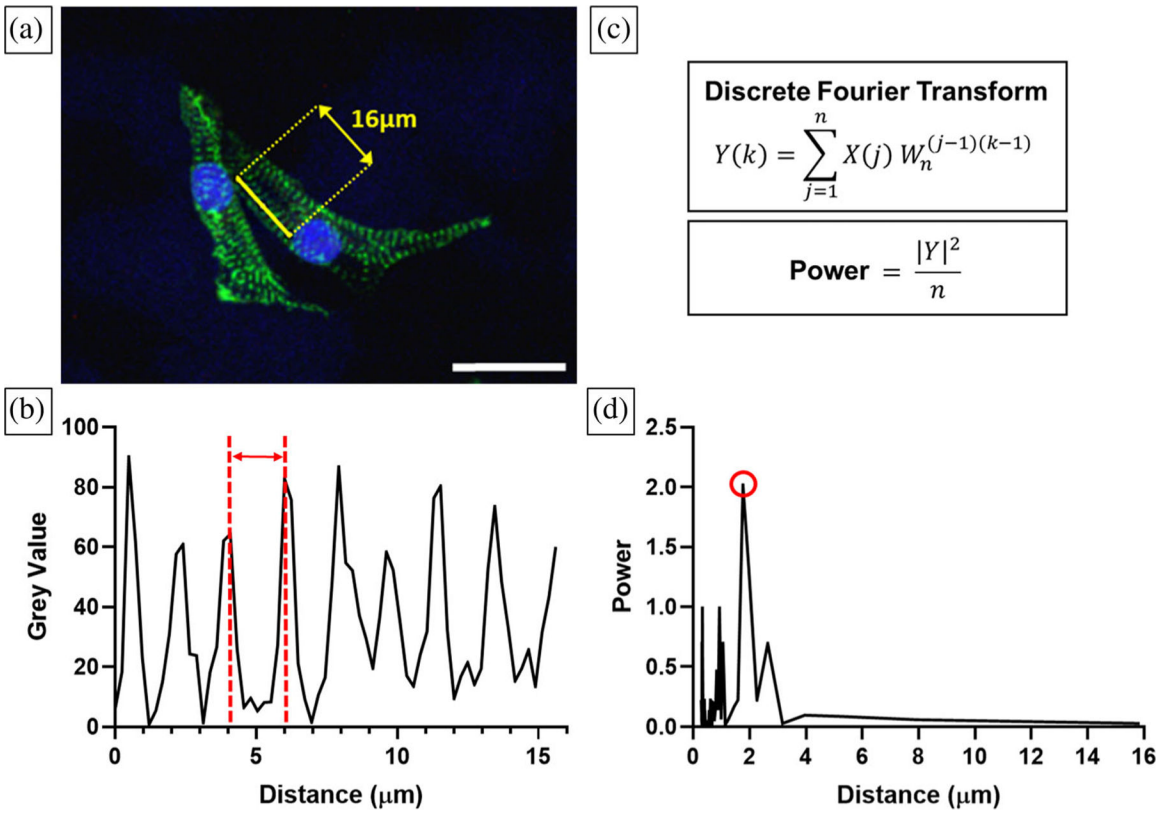

FIGURE 2.

Fourier transform analysis to calculate sarcomere lengths on decellularized leaves. (a) A 16 µm line (yellow) was drawn in ImageJ perpendicular to hiPS-CM α-actinin positive bands (green); nuclei (blue). Scale bar 25 µm. (b) Grey values plotted across the length of the line as shown in (a). Grey value peaks correspond to α-actinin positive regions, and the distance between these peaks (red) is the sarcomere length. (c) Sarcomere lengths were calculated with discrete fourier transform and power spectrum analysis. (d) Cell sarcomere length is equal to the distance value corresponding to the highest power, circled in red

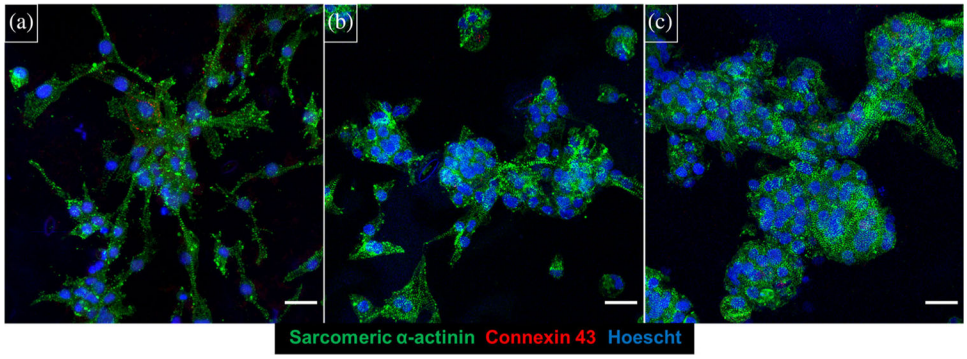

FIGURE 3.

hiPS-CMs cultured on decellularized spinach leaves. Cells cultured for 21 days on (a) collagen IV coated decellularized leaf, (b) fibronectin coated decellularized leaf, and (c) noncoated decellularized spinach leaf. Samples were stained for sarcomeric α-actinin (green), connexin-43 (red), and Hoescht 33342 (blue). Scale bar 25 μm

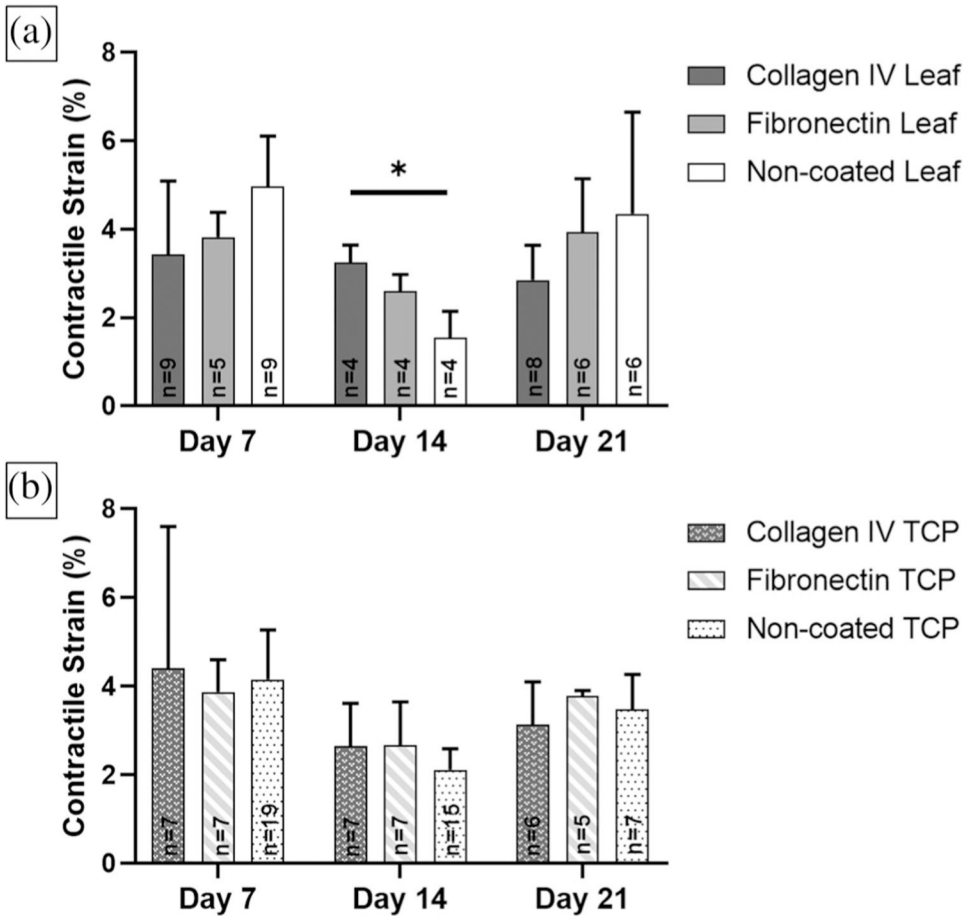

FIGURE 4.

Maximum contractile principle strain analysis for hiPS-CMs on ECM coated and noncoated decellularized spinach leaves for 7, 14, and 21 days. Sample sizes *n* for each condition are noted within the data. (a) There were no significant differences over time for coated and noncoated leaves. However, collagen IV coated leaves had larger contractile strain than noncoated leaves at Day 14 ($p < .05$). No significance difference was found between coated and noncoated leaves at days 7 and 21. (b) No significant differences were found in contractile strain for hiPS-CMs seeded on ECM coated and noncoated tissue culture plastic (TCP) at 7, 14, and 21 days. (a, b) There were no significant differences between coated and noncoated leaves and tissue culture plastic

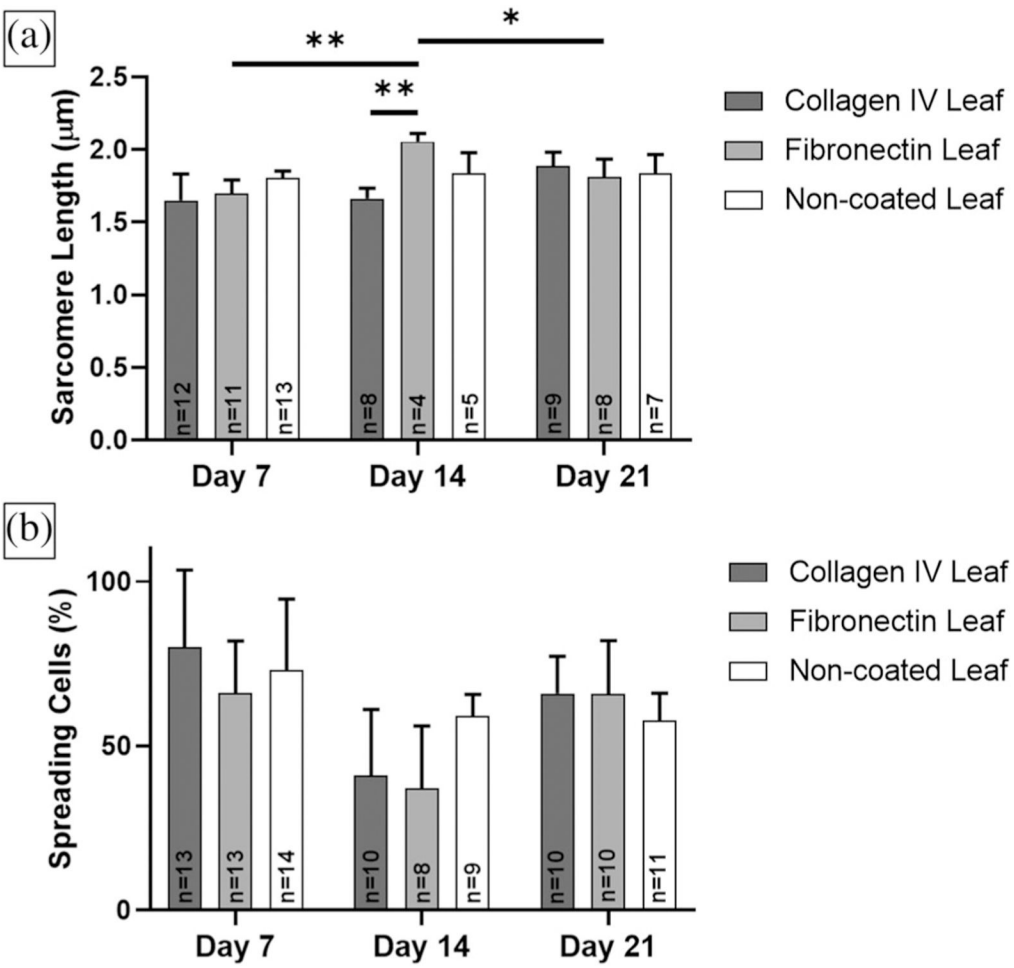

FIGURE 5.

Sarcomere length and cell spreading analysis for hiPS-CMs on ECM coated and non-coated decellularized spinach leaves for 7, 14, and 21 days. Sample sizes *n* for each condition are illustrated within the data. (a) Fibronectin coated leaves had statistically longer sarcomere lengths than collagen IV coated leaves at Day 14 ($p < .01$). Significant difference was also found in fibronectin coated leaves between Day 7 and 14 ($p < .01$), and Day 14 and 21 ($p < .05$). (b) There were no significant differences in cell spreading between culture time or coatings

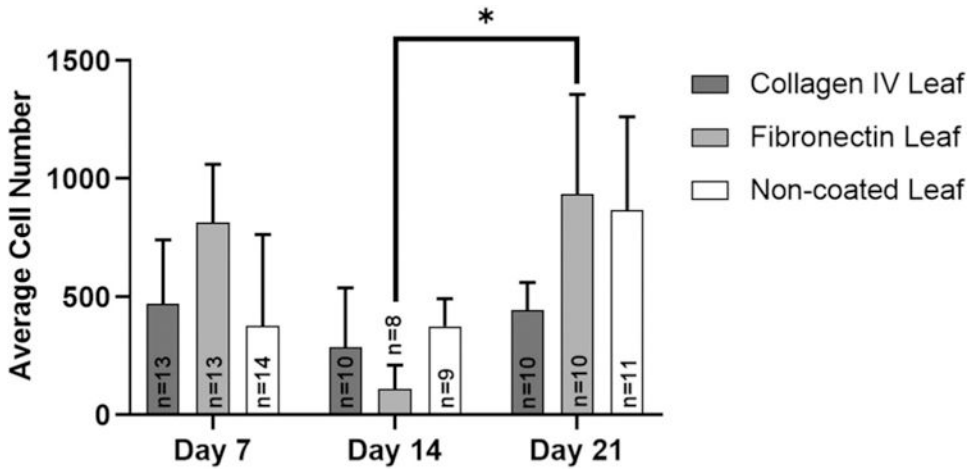

FIGURE 6.

Average cell number per mm^2 of IF sarcomeric α-actinin positive hiPS-CMs on coated and noncoated leaves over time. Sample sizes *n* for each condition are illustrated within the data. Fibronectin coated leaves had statistically less cells at Day 14 compared to Day 21 ($p < .05$)